

# Simultaneous TG/DTG–DSC–FTIR characterization of collagen in inert and oxidative atmospheres

Andrei Cucos · Petru Budrugaec

Received: 11 January 2013 / Accepted: 1 March 2013 / Published online: 26 March 2013  
© Akadémiai Kiadó, Budapest, Hungary 2013

**Abstract** In this paper, a TG/DTG–DSC–FTIR study of type I collagen extracted from bovine Achilles tendon both in inert (nitrogen) and oxidative atmosphere (synthetic air and oxygen) from room temperature to 700 °C was performed. The thermal analysis results have shown that after initial dehydration, collagen exhibits a single decomposition step in nitrogen (due to pyrolysis), while in air and oxygen two steps are observed due to thermo-oxidative decomposition, the latter being highly exothermic. The CO<sub>2</sub> bands dominate the FTIR spectra of evolved gases in all atmospheres (especially in air and oxygen), along with the characteristic bands of ammonia, water, HNCO, methane. In nitrogen, the bands of pyrrole, HCN, and ethane were also identified, while in oxidative atmospheres, nitrogen oxides and CO are released. A study was also performed by comparing the DTG and gas evolution curves observed for the three atmospheres.

**Keywords** Collagen · Thermal decomposition · TG–FTIR · Evolved gases

## Introduction

Collagen is the most abundant structural protein in mammals, being found in skin, cornea, cartilage, muscle, tendon, ligament, and bone. The basic building block of collagen is

the triple helix formed of three polypeptide chains coiled together, which further aggregates in structural levels of increasing complexity: microfibrils, fibrils, fibers, and tissue [1]. The unique physico-chemical properties of collagen are very sensitive to heating, as it may dehydrate, denature or decompose. The understanding of processes that collagen undergoes on heating and that may lead to alteration of collagen properties is crucial for its medical applications, such as reconstructive surgery, wound care, etc.

Collagen and collagen-based materials (films, sponges, scaffolds, parchments, leathers, bones) in dry (non-hydrated) state were characterized through numerous thermal analysis techniques. Some recent papers deal with TG/DTG [2–14], DSC [2, 3, 6, 9, 10, 14–17], dynamic mechanical analysis [2, 17], dielectric techniques [18], micro-thermal analysis [19], etc.

Evolution of gaseous products resulted from thermal decomposition/pyrolysis of some collagen-based materials was studied in several works by mass spectrometry [20–24].

On the other hand, TG–FTIR has become an increasingly used technique for characterizing biomaterials such as: amino acids [25–27], dipeptides [26, 28], casein protein [29], keratin-based materials like down powder [30], sheep wool, human hair, and chicken feathers [31], cellulose [32], wood lignin [33], latex [34], biomass residues [35], but also microalgae [36], mushrooms [37], etc. However, to our knowledge, no TG–FTIR study has yet been reported for collagen. The significance of such a study would reside in the fact that, on decomposition of complex systems such as proteins, FTIR analysis of the evolved gases could discriminate between the possible molecules of same molecular mass which were identified by MS, due to their different absorption bands in FTIR. Moreover, by complementing this study with DSC technique and by performing it in inert and oxidative atmospheres, some

---

A. Cucos (✉) · P. Budrugaec  
National Institute for Research and Development in Electrical Engineering ICPE-CA, Splaiul Unirii 313, 030138 Bucharest, Romania  
e-mail: andreicucos@icpe-ca.ro

pathways of collagen decomposition and oxidation can be elucidated. Thus, in this article, we have focused on a simultaneous TG/DTG–DSC–FTIR study of type I collagen extracted from bovine Achilles tendon.

## Materials

Type I collagen extracted from bovine Achilles tendon was purchased from Sigma-Aldrich. It was washed several times with absolute ethanol for removing fats and then allowed to dry and rehydrate at room temperature in air for several days.

## Methods

The TG/DTG/DSC + FTIR measurements were performed on a Netzsch STA 409 PC thermal analyzer coupled to a Bruker Tensor 27 FTIR spectrometer equipped with a TG-IR gas cell.

Fibrous collagen was pressed in a pellet, which was cut in small pieces, from which approx. 20 mg were placed in a cylindrical  $\text{Al}_2\text{O}_3$  holder and heated in nitrogen, synthetic air or oxygen flow ( $100 \text{ ml min}^{-1}$ , purity 99.999 %), from room temperature to  $700 \text{ }^\circ\text{C}$ , at a heating rate of  $10 \text{ }^\circ\text{C min}^{-1}$ . The adapter head, the transfer line, and the TG-IR cell were maintained at  $200 \text{ }^\circ\text{C}$  to avoid condensation of the evolved gases. The FTIR spectra were collected continuously during measurements in the wavenumber range  $4,000\text{--}650 \text{ cm}^{-1}$  at a resolution of  $4 \text{ cm}^{-1}$ .

## Results and discussion

### Nitrogen atmosphere

The recorded curves in nitrogen atmosphere are represented in Fig. 1. The TG and DTG curves are typical for collagen materials such as films, sponges, and scaffolds [2–6].

Thus, the first mass loss, which occurs from room temperature to about  $180 \text{ }^\circ\text{C}$  (DTG peak at  $96 \text{ }^\circ\text{C}$ ), and the corresponding broad endothermic DSC peak centered at  $105 \text{ }^\circ\text{C}$  are due to the loss of moisture. In the Gram–Schmidt curve, a weak broad peak with a maximum at  $118 \text{ }^\circ\text{C}$  is observed. The difference observed between the positions of DTG and Gram–Schmidt peaks is due to the time needed for the evolved gaseous species to reach the FTIR cell.

The second mass loss which is the major one and starts at above  $200 \text{ }^\circ\text{C}$  is due to the pyrolytic decomposition of collagen. A single large DTG peak is observed at  $330 \text{ }^\circ\text{C}$ . In the Gram–Schmidt curve, a large maximum is seen at

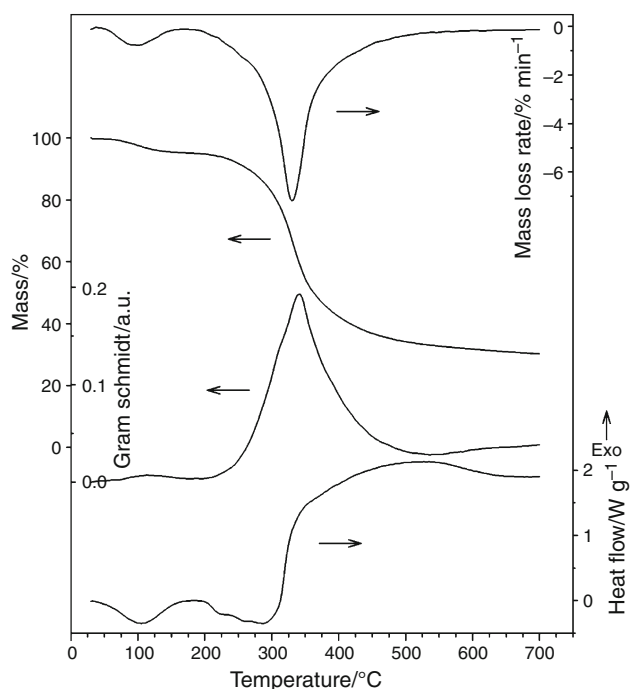


**Fig. 1** TG, DTG, DSC, and Gram–Schmidt curves of collagen in nitrogen atmosphere

$343 \text{ }^\circ\text{C}$ . At high temperatures, the mass continues to be lost, while in the Gram–Schmidt curve, a slight increase is observed, suggesting that gaseous products continue to evolve due to decomposition and internal oxidation of residues.

In the DSC curve, the second endothermic peak with a minimum at  $220 \text{ }^\circ\text{C}$  is attributed to denaturation of collagen, then a main endothermic process is observed at  $\sim 290 \text{ }^\circ\text{C}$  (pyrolytic decomposition), followed by a very broad exothermic process due to internal oxidation of residues. These features were also observed previously [2, 3, 6, 15–17].

The 2D and 3D plots of FTIR spectra of evolved gases (Fig. 2) give important information on thermal degradation of collagen and were interpreted according to the public NIST database [38]. The evolution curves of the main gaseous products (based on their strongest infrared band) are represented in Fig. 3.

Thus, in the first stage, the release of moisture water (series of narrow bands at  $4,000\text{--}3,500, 2,000\text{--}1,300 \text{ cm}^{-1}$ , Fig. 2) is evident.

On subsequent heating, a further and more intense evolution of  $\text{H}_2\text{O}$  is observed, reaching a maximum at  $337 \text{ }^\circ\text{C}$ , then a continuous and rather constant release is observed at high temperatures, due to decomposition and condensation reactions.

Ammonia, identified by a series of narrow bands at  $1,200\text{--}750 \text{ cm}^{-1}$  with the characteristic bands at  $964, 930$  (main bands),  $1,626$  and  $3,335 \text{ cm}^{-1}$  starts to evolve above

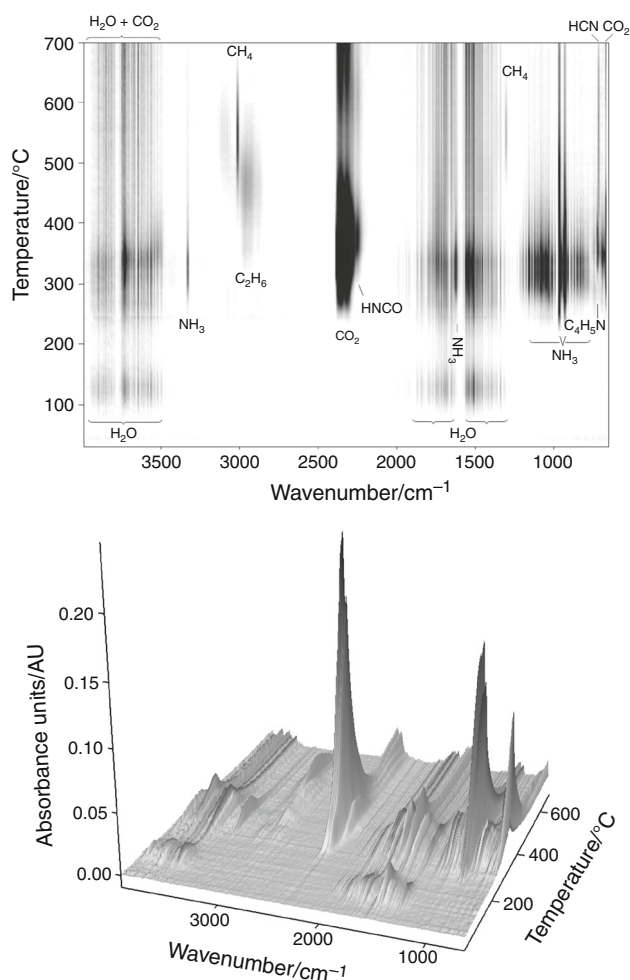


**Fig. 2** 2D (top) and 3D (bottom) plots of FTIR spectra of evolved gases from the decomposition of collagen in nitrogen atmosphere. In the 2D plot, a darker tint indicates a higher intensity

200 °C. Between 250 and 330 °C, its bands are the most intense (Fig. 3), suggesting that deamination might be the dominant decomposition process in this temperature region.

Ammonia originates from deamination reactions of collagen involving free  $-\text{NH}_2$  groups from arginine and lysine (51 and 25 residues/1,000 residues [39]) and peptide  $-\text{NH}-$  groups. After reaching a maximum release split at 325 and 340 °C, the intensity of  $\text{NH}_3$  bands diminishes and then slightly decreases at high temperatures. It is noteworthy to mention that nitrogen can also be released from collagen as  $\text{N}_2$  which is not detectable by FTIR.

The most intense band in the 2D and 3D FTIR plots is that of  $\text{CO}_2$  (2,200–2,400  $\text{cm}^{-1}$  with main peak at 2,358  $\text{cm}^{-1}$ ) which becomes visible at around 250 °C and sharply increases up to 350 °C. Minor  $\text{CO}_2$  bands are also observed. After falling to a broad minimum at 550 °C, a slight increase is observed at high temperatures. Carbon dioxide can originate from direct decarboxylation

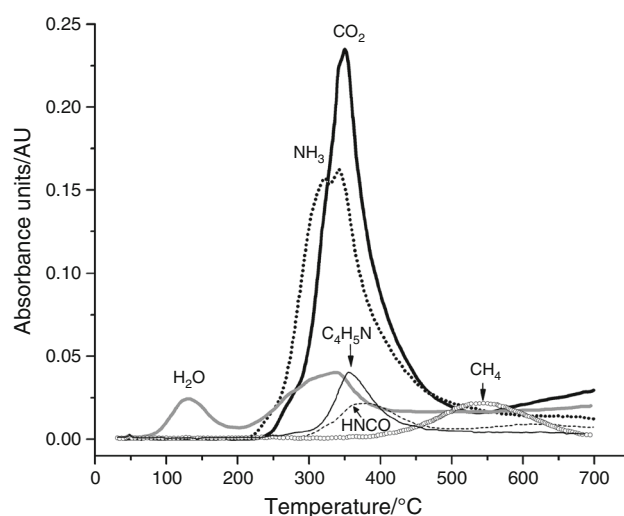


**Fig. 3** The evolution curves of the main gaseous products from the decomposition of collagen in nitrogen atmosphere

of free  $-\text{COOH}$  groups from glutamic and aspartic acids, which are found in significant proportions in bovine tendon collagen (77 and 46 residues/1,000 residues, respectively) [39]. We believe that this reaction is responsible for the incipient release of  $\text{CO}_2$ . Afterward,  $\text{CO}_2$  may be produced by condensation reactions involving peptide  $-\text{CO}-$  groups and by internal oxidation of other organic groups. The final slight increase in  $\text{CO}_2$  evolution must be due exclusively to condensation reactions within the residues (tar).

Above 300 °C, the evolution of  $\text{HNCO}$  (2,250  $\text{cm}^{-1}$ ) can be detected (maximum at 380 °C). However, the corresponding band is partially superimposed on the strong  $\text{CO}_2$  band, resulting in an augmented intensity.

Pyrrole ( $\text{C}_4\text{H}_5\text{N}$ ) was detected to evolve above 250 °C, with a peak at 355 °C, but its band (720  $\text{cm}^{-1}$ ) partially overlaps with a minor band of  $\text{CO}_2$ . Pyrrole was previously detected by Py-GC/MS as a major compound from pyrolysis of calf- and pig-skin collagen [21], leathers [21, 22], and bones [23, 24]. Pyrrole originates from proline [40], which is the second most abundant amino acid in collagen after glycine [39].

At above 370 °C, a band corresponding to  $\text{HCN}$  (714  $\text{cm}^{-1}$ ) appears, reaching a very broad maximum between 420 and 580 °C.

At higher temperatures, a broad band at 2,850–3,000  $\text{cm}^{-1}$ , with a highest peak at 2,968  $\text{cm}^{-1}$  reaching a maximum release at around 450 °C, was attributed to hydrocarbons, mainly ethane. On heating bone collagen in argon, a fragment mass of 30 was detected with a maximum release at 450 °C [12], being interpreted by the authors as  $\text{NO}$ ,  $\text{CH}_2\text{O}$  or  $\text{C}_2\text{H}_6$ . The coincidence of temperatures of maximum evolution, and the absence of detectable  $\text{NO}$  and  $\text{CH}_2\text{O}$  bands in our FTIR spectra

suggest that ethane may be responsible for this gaseous release.

Above 400 °C, the characteristic narrow peaks of CH<sub>4</sub> (3,016 and 1,304 cm<sup>-1</sup>) can be easily observed, which have a maximum intensity at around 550 °C. Methane may form by condensation reaction involving -CH<sub>3</sub> and -CH<sub>2</sub>- groups. It is interesting to note that the maximum CH<sub>4</sub> release coincides with a slight minimum in CO<sub>2</sub> evolution.

The above-mentioned compounds (except pyrrole) were also detected on thermal decomposition of another protein, casein [29].

Other compounds which were observed on thermal decomposition of collagen-based materials by MS [20–24] could not be clearly distinguished in our FTIR study due to the fact that their absorption bands are overlapped on the infrared bands of the above-mentioned gases.

#### Air atmosphere

In air atmosphere, the TG, DTG, and DSC curves recorded in our work closely resemble those reported for bovine Achilles tendon collagen by Lozano et al. [14]. Thus, three mass losses are observed (Fig. 4). The first one is due to dehydration, while the second and the third ones (DTG peaks at 308 and 607 °C, respectively) are due to decomposition through thermo-oxidation and are comparable. As in [14], we observed that at 700 °C all collagen is decomposed, however, a small amount of inorganic residue (originating from bovine tendon) remains.

In the DSC curve, the dehydration and denaturation endothermic peaks are observed at 102 and 221 °C, respectively, then oxidation starts above 250 °C, reaching a broad maximum at around 330 °C (corresponding to the 2nd mass loss step). The decomposition is further characterized by a series of exothermic processes, culminating with a very strong peak at 614 °C (3rd step) suggesting the intense oxidation of the residues formed in the previous stage. These features were also observed in [14].

The Gram–Schmidt curve exhibits three main peaks, as the DTG one, namely a very weak and broad peak at 118 °C due to dehydration, a medium peak at 332 °C and a large one with a maximum at 625 °C, illustrating the strong release of oxidation products. The differences of the relative intensities of Gram–Schmidt and DTG peaks could be due to different infrared absorptions of the evolved gases.

The FTIR spectra reveal the release of moisture water in the first stage (Fig. 5, 6). At above 220 °C, the formation of CO<sub>2</sub>, NH<sub>3</sub>, and H<sub>2</sub>O is observed. CO<sub>2</sub> is the main decomposition product in this stage and its evolution exhibits a peak at 330 °C. Pyrrole could not be detected, due to the interference with a CO<sub>2</sub> band. At above 280 °C, HNCO starts to evolve, together with small amounts of CO (two broad and weak bands at ~2,180 and ~2,115 cm<sup>-1</sup>).

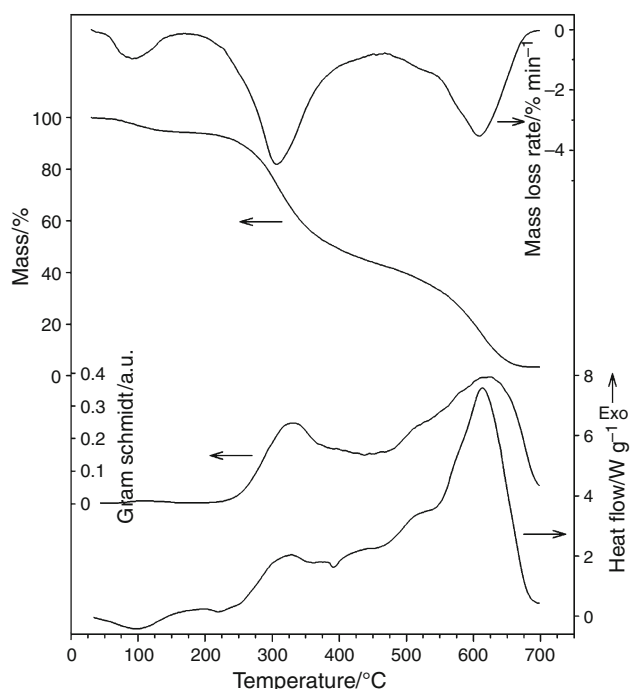


**Fig. 4** TG, DTG, DSC, and Gram–Schmidt curves of collagen in synthetic air

The ethane band is much weaker than in nitrogen and its release has apparently two maxima at around 350 and 500 °C.

For the 3rd step, several features are observed and firstly the strong increase of CO<sub>2</sub> band reaching a large maximum at 620 °C, due to the oxidation of organic residues. The formation of NO (two bands at 1,909 and 1,850 cm<sup>-1</sup>) and small amounts of NO<sub>2</sub> (band at 1,632 cm<sup>-1</sup>) through the oxidation of N-containing residues is noticed. NO evolution has a maximum at around 600 °C (a minor release could also be detected at around 400 °C, Fig. 6). It is noteworthy to mention that NO formation was previously observed on thermal decomposition of parchment, a collagen-based material, in an oxidative atmosphere (80 % Ar–20 % O<sub>2</sub>) by MS, with a minor peak at around 370 °C and a major one at ~530 °C [20]. These results suggest that nitrogen contained in collagen is mainly released in the form of NH<sub>3</sub> in the 2nd step and as NO in the 3rd step.

Methane starts to evolve at above 420 °C, reaching a maximum at 510 °C. Some amounts of water, NH<sub>3</sub>, and HNCO are also observed to be released at high temperatures.

#### Oxygen atmosphere

As expected, the decomposition of collagen in oxygen has much similarity with that in air. However, there are some minor but important differences. Thus, the 2nd and 3rd mass losses occur at lower temperature, as well as the complete decomposition, and the corresponding DTG

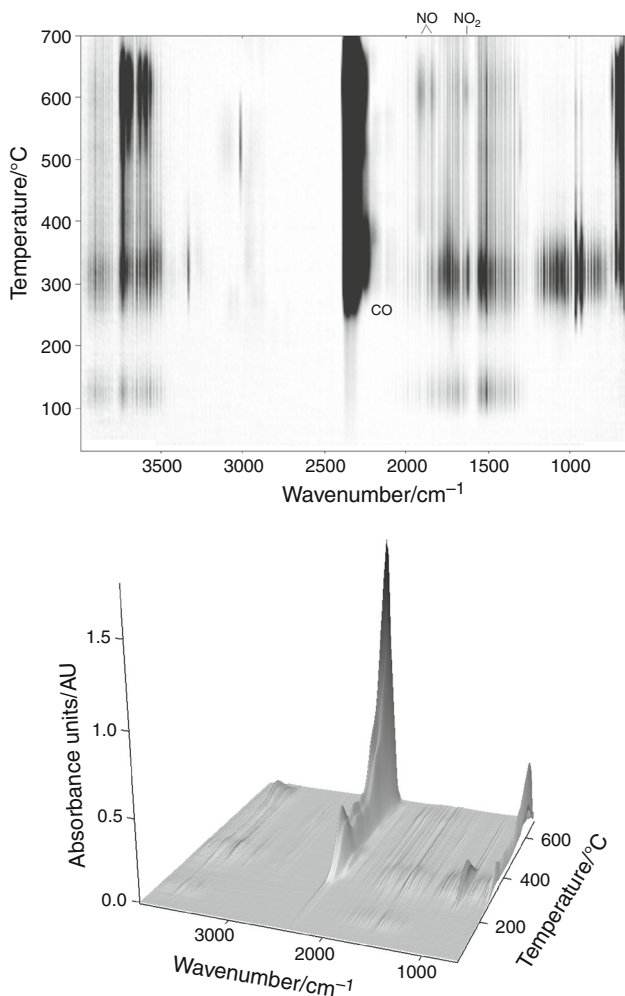


**Fig. 5** 2D (top) and 3D (bottom) plots of FTIR spectra of evolved gases from the decomposition of collagen in synthetic air. Attribution of other bands is as in Fig. 2. In the 2D plot, a darker tint indicates a higher intensity

peaks have a more complicated shape (Fig. 7): the 2nd DTG peak (275 °C) has a shoulder, while the 3rd DTG peak is even split in two (484 and 521 °C), with an additional shoulder at high temperatures. The same features are also observed in the DSC curve and, less pronounced, in the Gram–Schmidt curve. These facts confirm that the oxidation of collagen is easier but also more segregated in oxygen.

The FTIR spectra of evolved gases are represented in Fig. 8, while the evolution profiles of the main gases are given in Fig. 9. Thus, in the second decomposition step, among CO<sub>2</sub>, NH<sub>3</sub>, H<sub>2</sub>O, and HNCO as main gaseous products, the evolution of some amounts (larger than in air) of CO is observed.

The most important feature is observed in the 3rd decomposition step, namely the formation of three nitrogen oxides:

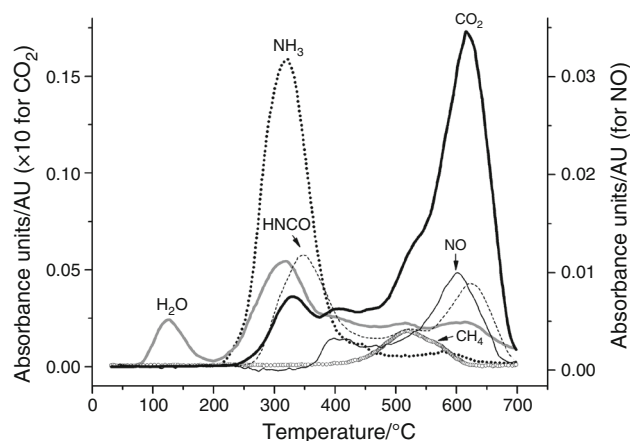


**Fig. 6** The evolution curves of the main gaseous products from the decomposition of collagen in synthetic air. NO curve was obtained by subtracting of H<sub>2</sub>O curve from the 1,909 cm<sup>-1</sup> evolution curve

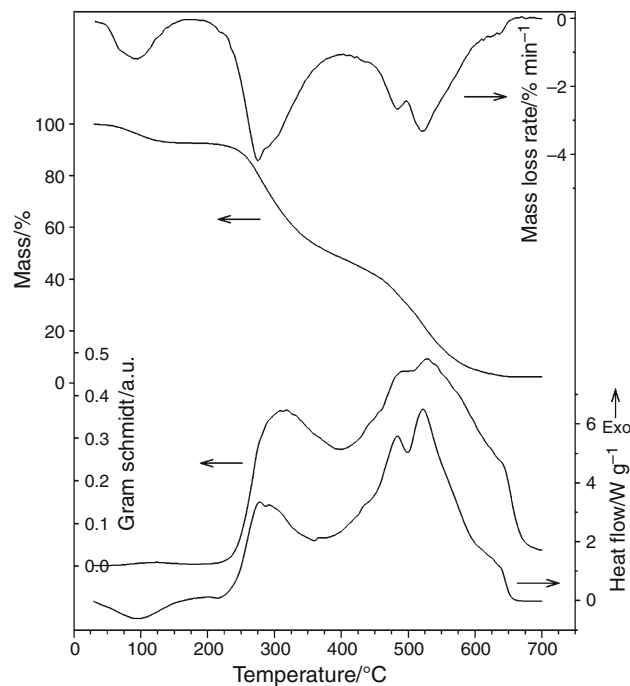


**Fig. 7** TG, DTG, DSC, and Gram–Schmidt curves of collagen in oxygen atmosphere

- NO<sub>2</sub> (1,630 and 1,595 cm<sup>-1</sup>) at above 450 °C, with a maximum release at ~560 °C,
- NO (1,910 and 1,850 cm<sup>-1</sup>), maximum evolution at ~550 °C,
- N<sub>2</sub>O (two main bands at 2,243 and 2,205 cm<sup>-1</sup> and two minor ones at 1,313 and 1,269 cm<sup>-1</sup>) with maximum release at 520 °C and a minor one at ~640 °C.

As in air, these oxides must originate from the oxidation of N-containing residues. N<sub>2</sub>O was previously observed on combustion of some mushrooms in air [37].



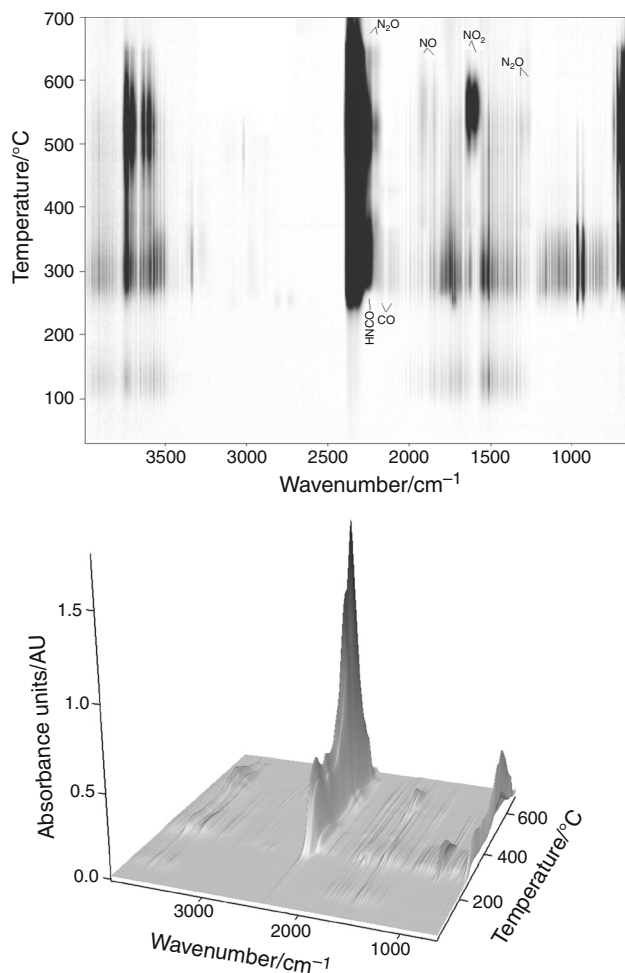


**Fig. 8** 2D (*top*) and 3D (*bottom*) plots of FTIR spectra of evolved gases from the decomposition of collagen in oxygen atmosphere. Attribution of other bands is as in Fig. 5. In the 2D plot, a *darker tint* indicates a higher intensity

The peak of methane at 500 °C has a much reduced intensity than in nitrogen or air atmosphere, while the hydrocarbons/ethane band is not more visible.

#### Comparison of DTG and gas evolution curves

As it can be seen in Fig. 10, the dehydration step in the three atmospheres is characterized by similar peaks. The positions of the peaks are essentially the same and differences in their height could be due to some variations in moisture content as a result of sample preparation and in situ dehydration in the STA instrument prior to the start of measurements.

The major difference is seen in the 2nd step. Thus, the DTG peak is the highest for N<sub>2</sub>, but is also at the highest temperature. In air and O<sub>2</sub>, the maximum rates of mass loss are similar; however, the peak in O<sub>2</sub> is at lower temperature and has a shoulder. These data suggest that:

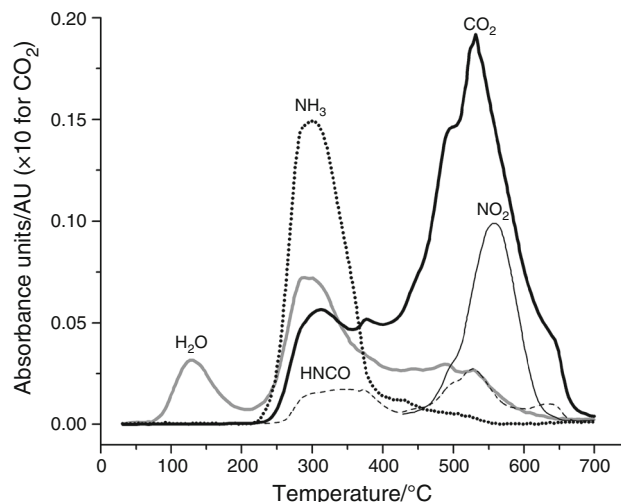


**Fig. 9** The evolution curves of the main gaseous products from the decomposition of collagen in oxygen atmosphere. NO<sub>2</sub> curve was shown from 425 °C, as at lower temperatures the bands of NH<sub>3</sub> appear at this wavenumber

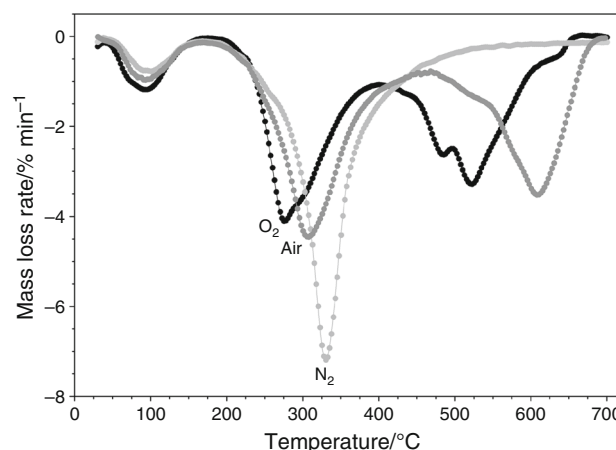


**Fig. 10** The DTG curves of collagen in the three atmospheres used in this study

- in N<sub>2</sub>, the second mass loss is due to the decomposition and internal oxidation, with a rapid formation and release of volatile compounds;
- in air, the external oxidation leads to a decrease of decomposition temperature, but the rate of mass loss is also lower due to the fact that O-containing products are formed slower than the residues in nitrogen atmosphere.
- in O<sub>2</sub>, the DTG peak is shifted to even lower temperature, due to the more facile oxidation of collagen.

The 3rd step which does not exist in N<sub>2</sub> atmosphere is characterized by a broad DTG peak in air and O<sub>2</sub>. The heights of the peaks are also quite similar, and in O<sub>2</sub>, the

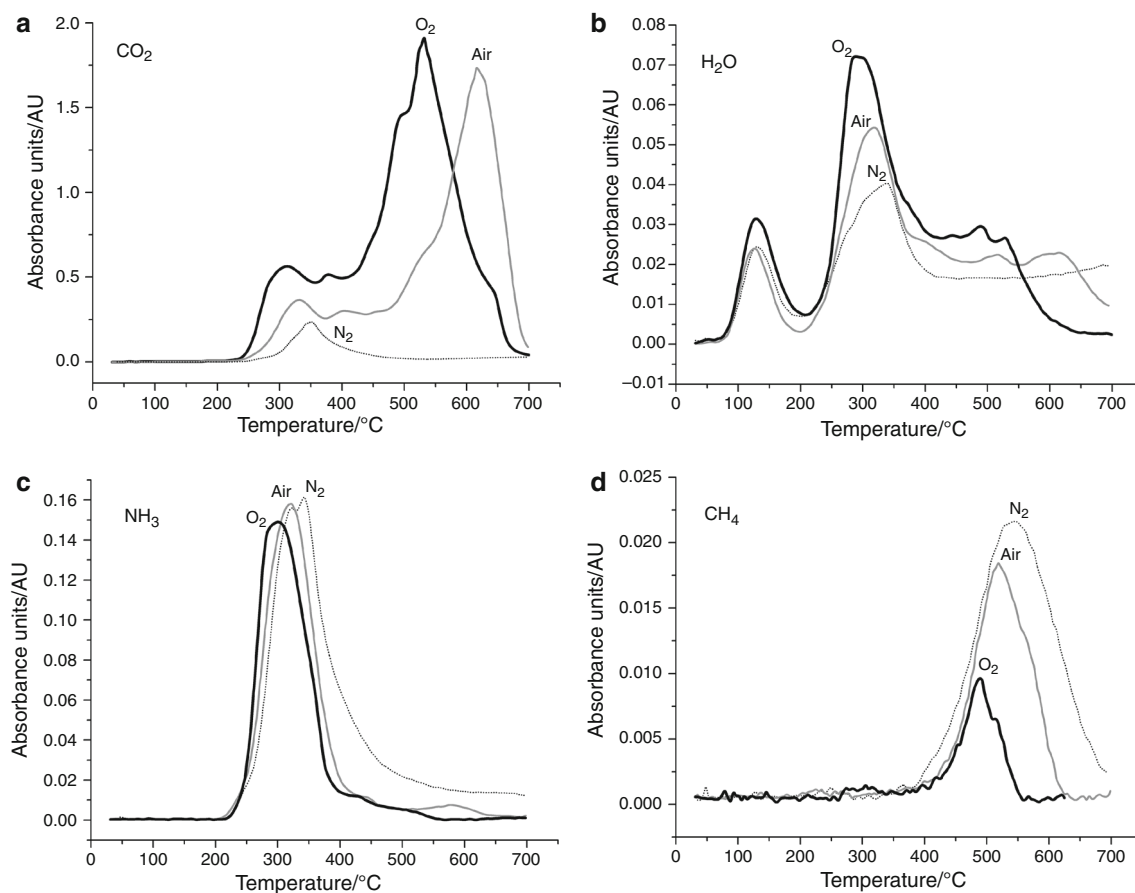


**Fig. 11** Evolution curves of CO<sub>2</sub>, H<sub>2</sub>O, NH<sub>3</sub> and CH<sub>4</sub> which are formed in all three atmospheres (N<sub>2</sub>, air, O<sub>2</sub>)

peak is much shifted to lower temperature, the shifting being larger ( $\sim 80$  °C) than in the previous step ( $\sim 30$  °C) suggesting that the residues formed in the 2nd step are much easier oxidized in O<sub>2</sub> than in air. Also, in O<sub>2</sub>, the DTG peak is split in two, while in air only a shoulder is observed at lower temperature, indicating that in this step there are two main processes that are better resolved in O<sub>2</sub>.

The evolution profiles of the gases (CO<sub>2</sub>, H<sub>2</sub>O, NH<sub>3</sub> and CH<sub>4</sub>) which are formed in all three atmospheres are represented in Fig. 11.

In nitrogen, the single CO<sub>2</sub> evolution peak is due, as was previously mentioned, to decarboxylation of free –COOH groups (from aspartic and glutamic acids), to condensation reactions involving peptide –CO– groups and to internal oxidation of other organic groups. In air and oxygen, the CO<sub>2</sub> evolution curves have similar shapes (Fig. 11a), and some observations must be mentioned. First, on increasing oxygen content of atmosphere, a progressive increase of CO<sub>2</sub> evolution peak for the 2nd TG step and a shifting to lower temperatures is observed. This can be explained by the fact that in an oxidative atmosphere CO<sub>2</sub> is mainly produced by external oxidation of organic groups and condensation reactions, while direct decarboxylation

remains as a minor source of CO<sub>2</sub>. In the 3rd step, the intense oxidation of residues formed in the previous step leads to large peaks in CO<sub>2</sub> evolution, which also increase (slightly) and shift (by  $\sim 90$  °C) to lower temperatures from air to oxygen atmosphere.

In the case of water, a similar trend is observed (Fig. 11b), except the first dehydration peak, which occurs at the same temperature. Its height slightly differs for the three atmospheres, due to the previously discussed causes. The most important difference is observed for the second peak corresponding to the 2nd mass loss. Thus, in nitrogen atmosphere, water may originate mainly from intra and intermolecular condensation, and internal oxidation, while in air and O<sub>2</sub>, more supplementary water is produced by external oxidation. Consequently, the H<sub>2</sub>O peak rises in height and shifts at lower temperature with the increase of oxygen content of atmosphere. On further heating in nitrogen, water is continuously removed from condensation reactions within residues, while in air and oxygen at least two distinct and weaker peaks are observed (shifted to lower temperatures in the latter case) followed by a diminishing of water evolution, indicating the end of combustion.

Ammonia originates, as mentioned above, from deamination reactions of the protein involving free  $\text{-NH}_2$  groups and peptide  $\text{-NH-}$  groups and is the main N-containing decomposition product of collagen at below  $400\text{ }^\circ\text{C}$ , as was observed for all three atmospheres. In nitrogen, a splitting of the evolution peak and a continuous release at high temperatures (due to internal condensations) is observed (Fig. 11c). In air and oxygen, the shifting of peaks to lower temperature suggests a more facile deamination. In fact, the oxidation of collagen causes the destruction of covalent bonds in the molecule and, respectively, an easier release of ammonia. The intensities of the peaks seem to follow a descendent trend and, after reaching these maxima, the  $\text{NH}_3$  evolution decreases faster than in nitrogen. Also, in air, a small peak corresponding to the 3rd mass loss is observed, while in oxygen only a shoulder at  $\sim 500\text{ }^\circ\text{C}$  is visible. All these data suggest that in an oxidative atmosphere a fraction of nitrogen from N-containing products is oxidized and released as nitrogen oxides.

Finally, methane may be formed by condensation reaction involving methyl and methylene groups. It is obvious that in an inert atmosphere, its release will be maximum (Fig. 11d), while the oxidation of these groups in air and especially in oxygen will decrease the  $\text{CH}_4$  evolution and will lead to an artificial shifting of the peak to lower temperature.

## Conclusions

A TG/DTG–DSC–FTIR study of type I collagen extracted from bovine Achilles tendon in nitrogen, air, and oxygen was performed. The TG/DTG results have shown that in the studied temperature region (r.t.  $700\text{ }^\circ\text{C}$ ) collagen exhibits two decomposition steps in nitrogen (due to dehydration and pyrolysis, respectively), while in air and oxygen, three steps are observed due to dehydration and thermo-oxidative decompositions. For oxygen atmosphere, the 2nd and 3rd DTG peaks are shifted to lower temperatures compared to air, indicating a more facile oxidation. DSC data have shown an endothermic peak associated with dehydration at around  $100\text{ }^\circ\text{C}$ , a broad exothermic process at above  $300\text{ }^\circ\text{C}$  for collagen decomposition in nitrogen (due to internal oxidation reactions), and two main exothermic peaks (the latter being very intense) in air and oxygen, corresponding to the 2nd and 3rd mass losses, and which are due to external oxidation.

The  $\text{CO}_2$  bands dominate the FTIR spectra in all atmospheres, along with the characteristic bands of ammonia, water,  $\text{HNCO}$ , and methane. In nitrogen, the bands of pyrrole,  $\text{HCN}$ , and ethane were identified, while in oxidative atmospheres nitrogen oxides and  $\text{CO}$  are released.

A study was also performed by comparing the DTG and gas evolution curves observed for the three atmospheres.

These studies can provide important information about the mechanisms of processes taking place on thermal decomposition of collagen.

**Acknowledgments** This work was supported by a grant of the Romanian National Authority for Scientific Research, CNCS-UEFI-SCDI, Project Number PN-II-RU-PD-2011-3-0047.

## References

1. Fratzl P, editor. Collagen: structure and mechanics. New York: Springer; 2008. p. 49–80.
2. Pietrucha K. Changes in denaturation and rheological properties of collagen–hyaluronic acid scaffolds as a result of temperature dependencies. *Int J Biol Macromol*. 2005;36:299.
3. Davidenko N, Campbell JJ, Thian ES, Watson CJ, Cameron RE. Collagen–hyaluronic acid scaffolds for adipose tissue engineering. *Acta Biomater*. 2010;6:3957–68.
4. He L, Mu C, Shi J, Zhang Q, Shi B, Lin W. Modification of collagen with a natural cross-linker, procyanidin. *Int J Biol Macromol*. 2011;48(2):354–9.
5. Sionkowska A, Wisniewski M, Skopinska J, Poggi GF, Marsano E, Maxwell CA, Wess TJ. Thermal and mechanical properties of UV irradiated collagen/chitosan thin films. *Polym Degrad Stab*. 2006;91:3026–32.
6. Lungu A, Albu MG, Florea NM, Stancu IC, Vasile E, Iovu H. The influence of glycosaminoglycan type on the collagen-glycosaminoglycan porous scaffolds. *Dig J Nanomater Bios*. 2011;6(4):1867–75.
7. Horn MM, Amaro Martins VC, de Guzzi Plepis AM. Interaction of anionic collagen with chitosan: effect on thermal and morphological characteristics. *Carbohydr Polym*. 2009;77:239–43.
8. Budrugaec P, Miu L, Popescu C, Wortmann FJ. Identification of collagen-based materials that are supports of cultural and historical objects. *J Therm Anal Calorim*. 2004;77:975–85.
9. Popescu C, Budrugaec P, Wortmann FJ, Miu L, Demco D, Baias M. Assessment of collagen-based materials which are supports of cultural and historical objects. *Polym Degrad Stab*. 2008;93:976–82.
10. Badea E, Miu L, Budrugaec P, Giurginca M, Mašić A, Badea N, Della Gatta G. Study of deterioration of historical parchments by various thermal analysis techniques complemented by SEM, FTIR, UV–Vis–NIR and unilateral NMR investigations. *J Therm Anal Calorim*. 2008;91:17–27.
11. Onishi A, Thomas PS, Stuart BH, Guerbois JP, Forbes SL. Tg–Ms analysis of the thermal decomposition of pig bone for forensic applications. *J Therm Anal Calorim*. 2008;92(1):87–90.
12. Onishi A, Thomas PS, Stuart BH, Guerbois JP, Forbes SL. Tg–Ms characterisation of pig bone in an inert atmosphere. *J Therm Anal Calorim*. 2007;88(2):405–9.
13. Mkukuma LD, Skakle JMS, Gibson IR, Imrie CT, Aspden RM, Hukins DWL. Effect of the proportion of organic material in bone on thermal decomposition of bone mineral: an investigation of a variety of bones from different species using thermogravimetric analysis coupled to mass spectrometry, high-temperature X-ray diffraction, and fourier transform infrared spectroscopy. *Calcif Tissue Int*. 2004;75:321–8.
14. Lozano LF, Peña-Rico MA, Heredia A, Ocotlán-Flores J, Gómez-Cortés A, Velázquez R, Belío IA, Bucio L. Thermal analysis study of human bone. *J Mater Sci*. 2003;38:4777–82.



15. Budrugaec P, Miu L. The suitability of DSC method for damage assessment and certification of historical leathers and parchments. *J Cult Heritage*. 2008;9:146–53.
16. Budrugaec P, Badea E, Della Gatta G, Miu L, Comănescu A. DSC study of deterioration of parchment exposed to environmental chemical pollutants (SO<sub>2</sub>, NO<sub>x</sub>). *Thermochim Acta*. 2010;500:51–62.
17. Cucos A, Budrugaec P, Miu L, Mitrea S, Sbarcea G. Dynamic mechanical analysis (DMA) of new and historical parchments and leathers. Correlations with DSC and XRD. *Thermochim Acta*. 2011;516:19–28.
18. Samouillan V, Lamure A, Lacabanne A. Dielectric relaxations of collagen and elastin in the dehydrated state. *Chem Phys*. 2000;255:259–71.
19. Bozec L, Odlyha M. Thermal denaturation studies of collagen by microthermal analysis and atomic force microscopy. *Biophys J*. 2011;101:228–36.
20. Roudit B, Odlyha M. Prediction of thermal stability of fresh and aged parchment. *J Therm Anal Calorim*. 2006;85(1):157–64.
21. Kurata S, Ichikawa K. Identification of small bits of natural leather by pyrolysis gas chromatography mass spectrometry. *Bunseki Kagaku*. 2008;57(7):563–9.
22. Marcilla A, García AN, León M, Martínez P, Bañón E. Study of the influence of NaOH treatment on the pyrolysis of different leather tanned using thermogravimetric analysis and Py/GC–MS system. *J Anal Appl Pyrol*. 2011;92:194–201.
23. Lodowska J, Wolny D, Kurkiewicz S, Węglarz L. The Pyrolytic Profile of Lyophilized and Deep-Frozen Compact Part of the Human Bone. *Sci World J*. 2012(2012) Article ID 162406, 7 pages doi:10.1100/2012/162406.
24. Purevsuren B, Avid B, Gerelmaa T, Davaajav Ya, Morgan TJ, Herod AA, Kandiyoti R. The characterisation of tar from the pyrolysis of animal bones. *Fuel*. 2004;83:799–805.
25. Li J, Wang Z, Yang X, Hu L, Yuwen L, Wang C. Decomposing or subliming? An investigation of thermal behavior of L-leucine. *Thermochim Acta*. 2006;447:147–53.
26. Li J, Wang Z, Yang X, Hu L, Yuwen L. Evaluate the pyrolysis pathway of glycine and glycylglycine by TG–FTIR. *J Anal Appl Pyrol*. 2007;80:247–53.
27. Li J, Yuwen L, Jingyan S, Wang Z, Hu L, Yang X, Wang C. The investigation of thermal decomposition pathways of phenylalanine and tyrosine by TG–FTIR. *Thermochim Acta*. 2008;467:20–9.
28. Kruse J, Eckhardt K-U, Regier T, Leinweber P. TG–FTIR, LC/MS, XANES and Py-FIMS to disclose the thermal decomposition pathways and aromatic N formation during dipeptide pyrolysis in a soil matrix. *J Anal Appl Pyrol*. 2011;90(2):164–73.
29. Mocanu AM, Moldoveanu C, Odochian L, Paius CM, Apostolescu N, Neculau R. Study on the thermal behavior of casein under nitrogen and air atmosphere by means of the TG-FTIR technique. *Thermochim Acta*. 2012;546:120–6.
30. Liu X, Gu S, Xu W. Thermal and structural characterization of superfine down powder. *J Therm Anal Calorim*. 2013;111(1):259–66.
31. Brebu M, Spiridon I. Thermal degradation of keratin waste. *J Anal Appl Pyrol*. 2011;91:288–95.
32. Shen DK, Gu S. The mechanism for thermal decomposition of cellulose and its main products. *Bioresour Technol*. 2009;100:6496–504.
33. Liu Q, Wang S, Zheng Y, Luo Z, Cen K. Mechanism study of wood lignin pyrolysis by using TG–FTIR analysis. *J Anal Appl Pyrol*. 2008;82(1):170–7.
34. Agostini DLS, Constantino CJL, Job AE. Thermal degradation of both latex and latex cast films forming membranes. Combined TG/FTIR investigation. *J Therm Anal Calorim*. 2008;91(3):703–7.
35. Giuntoli J, de Jong W, Arvelakis S, Spliethoff H, Verkooijen AHM. Quantitative and kinetic TG-FTIR study of biomass residue pyrolysis: dry distiller's grains with solubles (DDGS) and chicken manure. *J Anal Appl Pyrol*. 2009;85:301–12.
36. Marcilla A, Gómez-Siurana A, Gomis C, Chápuli E, Catalá MC, Valdés FJ. Characterization of microalgal species through TGA/FTIR analysis: application to nanochloropsis sp. *Thermochim Acta*. 2009;484:41–7.
37. Tănase C, Odochian L, Apostolescu N, Pui A. TG–FTIR analysis applied to the study of thermal behaviour of some edible mushrooms. *J Therm Anal Calorim*. 2011;103:1079–85.
38. NIST Chemistry Webbook Standard Reference Database No. 69, June, 2005 Release (<http://webbook.nist.gov/chemistry>).
39. Stevens FS, Jackson DS. Purification and amino acid composition of monomeric and polymeris collagens. *Biochem J*. 1967;104:534–6.
40. Britt PF, Buchanan AC, Owens CV, Skeen J. Does glucose enhance the formation of nitrogen containing polycyclic aromatic compounds and polycyclic aromatic hydrocarbons in the pyrolysis of proline? *Fuel*. 2004;83:1417–32.